Laser-Hole Boring into Overdense Plasmas Measured with Soft X-Ray Laser Probing

K. Takahashi,[1] R. Kodama,[1] K. A. Tanaka,[1,*] H. Hashimoto,[1] Y. Kato,[1] K. Mima,[1] F. A. Weber,[2] T. W. Barbee, Jr.,[2] and L. B. Da Silva[2]

[1]*Institute of Laser Engineering, Osaka University, Yamada Oka 2-6, Suita, Osaka 565-0871, Japan*
[2]*University of California, Lawrence Livermore National Laboratory, P.O. Box 808, Livermore, California 94550*

(Received 2 August 1999)

A laser self-focused channel formation into overdense plasmas was observed using a soft x-ray laser probe system with a grid image refractometry (GIR) technique. 1.053 μm laser light with a 100 ps pulse duration was focused onto a preformed plasma at an intensity of 2×10^{17} W/cm^2. Cross sections of the channel were obtained which show a 30 μm diameter in overdense plasmas. The channel width in the overdense region was kept narrow as a result of self-focusing. Conically diverging density ridges were also observed along the channel, indicating a Mach cone created by a shock wave due to the supersonic propagation of the channel front.

PACS numbers: 52.35.Mw, 52.40.Nk, 52.50.Jm, 52.70.La

Recent progress in high intensity short pulse laser technology is opening possibilities of the fast ignitor concept in inertial confinement fusion (ICF) [1]. This concept requires efficient heating of an imploded fuel plasma by high intensity short pulse laser light. One of the scenarios for efficient energy deposition of the short pulse is a laser channel formation into the overdense region by using a relatively long (hundreds of picoseconds) and intense ($I\lambda^2 = 10^{17}$–10^{19} W μm^2/cm^2) laser pulse for guiding a heating short pulse. At these intensities, electron quiver motions dominate thermal motions and ponderomotive force changes the plasma profile. The ponderomotive force pushes the critical surface forward and evacuates plasmas radially in an inhomogeneous plasma, resulting in a channel formation into overdense regions [2]. The channel formation by the ponderomotive force in underdense plasmas was experimentally studied by optical probing [3–5]. A number of experiments report self-focusing of laser light, channel formation in underdense plasmas, and the enhancement of the laser power in the channel [6,7]. Measurement of a Doppler shift in backscattered spectra from the turning point has been applied to study hole boring into an overdense region [8,9]. In this experiment, an observed large Doppler shift ($\Delta\lambda/\lambda \sim 10^{-3}$) and other supporting data suggested that a high intensity laser interacting with a preformed plasma caused self-focusing and penetrated into an overdense region. However, no direct measurement of the hole boring into overdense plasmas has been reported yet since it is impossible for a visible laser to probe the overdense region because of strong refraction and opacity.

A probe system using x-ray laser light is a powerful diagnostic tool in overdense plasmas because of the short wavelength and high brightness [10,11]. We have developed x-ray laser grid image refractometry (XRL-GIR) [12] to investigate the formation of laser channeling into overdense plasmas. Cross sections of the overdense region where self-focused laser light penetrated were obtained with the XRL-GIR system. We also present a laser channel into overdense plasmas and a conical density perturbation indicating a Mach cone created by a supersonic propagation of the channel front.

Experiments were carried out using the GEKKO XII laser system at the Institute of Laser Engineering, Osaka University. A plane plastic (CH) target with 100 μm thickness was irradiated obliquely by two 0.351 μm laser beams of 100 ps (FWHM) double pulses with a time separation of 400 ps to produce a preplasma at a 400 μm focal spot and a laser intensity of 10^{14} W/cm^2. A main pulse for channel formation at a wavelength of 1.053 μm was focused normally onto the preplasma at 1 ns after the first pulse of the 0.351 μm laser with a $f/3$ aspherical lens. The main pulse intensity was 2×10^{17} W/cm^2 with a 30 μm spot diameter at the best focus and the focal depth was 160 μm (± 80 μm) in vacuum condition. The best focus position was set at 210 μm away from the initial target surface, both infrared and blue laser pulses have temporally Gaussian shapes and 1:1 intensity ratios of the double pulses. The laser channel formation was measured with four diagnostics as shown in Fig. 1. Electron density profiles at 10^{19}–10^{20} cm^{-3} were measured

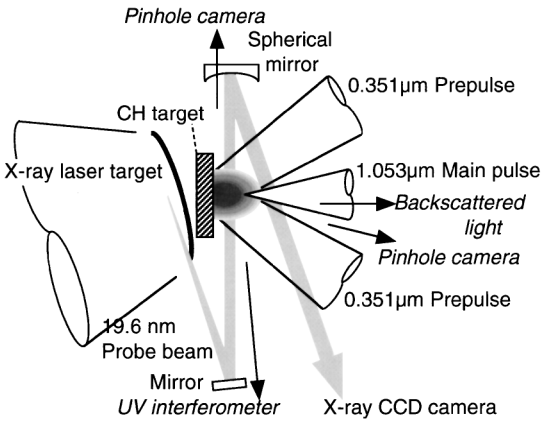

FIG. 1. Schematic of the experiment to study laser-hole boring.

by an UV interferometer system using 263 nm laser light with a 10 ps pulse duration [3]. Plasma behaviors at the laser turning point ($\sim 10^{21}$ cm^{-3}) were monitored by the measurement of a Doppler shift of the backscattered light spectra [8,9]. 1–30 keV x-ray images were obtained with x-ray pinhole cameras coupled to x-ray charge-coupled device (CCD) detectors from both front and side directions [13]. Electron density profiles were measured at 3×10^{20}–10^{22} cm^{-3} by an x-ray laser probe system. A GIR technique [12] was applied in this system to obtain two dimensional density profiles of laser channeling into overdense plasmas [14]. The XRL-GIR method measures the two dimensional deflection of the x-ray laser beam in a plasma. Since a fine mesh is inserted in the path of the x-ray laser beam, the imaged grid (mesh) passes through the plasma. The position of the grid image element is deflected toward lower density plasma because of dependence of the refractive index on the plasma density. Assuming the refractive index given by the electron plasma density (n_e) as $\eta = (1 - n_e/n_{\rm cr})^{1/2}$ ($n_{\rm cr}$: the critical electron density for the probe beam), electron density profiles of the plasma can be evaluated from the distorted grid image by using an iterative ray-tracing technique.

A Ne-like germanium (Ge) x-ray laser with a 19.6 nm wavelength [15] was used as a probe in the XRL-GIR system. A single beam of 1.053 μm laser light irradiated a 2.5 cm long Ge curved target set behind a CH target with a double pulse to generate a 19.6 nm x-ray laser pulse with an 80 ps pulse width. The temporal peak of the x-ray laser was set to probe the interaction plasma at 50 ps after the peak of the first channeling pulse. The CH target was used for the channel forming experiment. The x-ray laser beam was guided into the interaction region with a flat Mo/Si multilayer mirror as shown in Fig. 1. The x-ray probe was normal to the channel formation laser. The interaction region illuminated by the probe beam was relayed with a spherical multilayer mirror of 74 cm concave radius onto a back-illumination-type x-ray CCD camera with 12 times magnification [14]. The CCD was located at a distance of 80 cm away from the imaging point to enhance the grid distortion. A 213 μm pitch mesh as a grid was set 60 cm from the imaging point between the target and the imaging point [14]. This arrangement was optimized to probe a plasma with a scale length of 100 μm at 10^{20}–10^{22} cm^{-3} electron densities. The system had a spatial resolution less than 10 μm determined by a combination of the grid size and the magnification of the spherical mirror.

Figure 2(a) shows a side-on XRL-GIR image of the laser channel formation with the main pulse at an intensity of 2×10^{17} W/cm^2. The preplasma was created within a 400 μm diameter and the channeling beam was focused on the preplasma at a 210 μm distance away from the target surface along the center axis normal to the target. The white and the dark regions indicate no x-ray laser exposure and the x-ray laser signals through the grid, respectively, in Fig. 2(a). The x-ray laser beam was deflected to the lower electron density sides and the grid image was distorted accordingly. Up to 50 μm from the target surface, no grid image is seen because of strong refraction and absorption of the x-ray probe in the overdense plasma. Three types of grid distortions are seen on the image in addition to a distortion caused by the plasma expansion. One type is a ball-like (ball) structure having no grid points inside and a 40 μm diameter, which appears at 150 μm from the target surface. The second interesting distortions, which are the most important features in this paper, appeared along the main beam direction as pointed out by solid lines (S line). The third ones are grid distortions seen along the dotted lines (D line).

In the ball structure, the grid pattern is radially distorted and shifted toward the outside, indicating that the

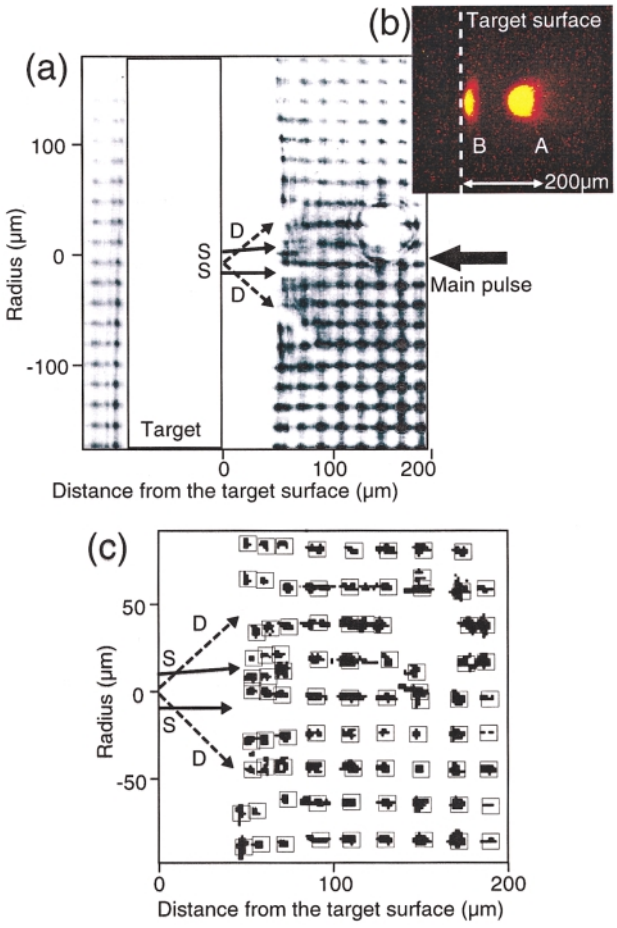

FIG. 2 (color). (a) XRL-GIR picture of the interaction region. The preplasma was created on the right hand side of the target and the channeling beam was injected from the right. (b) X-ray pinhole camera image observed at an angle almost the same as the one in (a). The angle was different by 45° from (a). The preplasma was created on the right hand side of the target and the channeling beam was injected from the right. (c) Magnified image of (a). The grid image is distorted because of deflection due to laser channeling, Mach cone, and a ball-like structure. The distorted grid image was contrast enhanced.

density decreases toward the outside. The ball corresponds to the density hump with a peak electron density of $6 \pm 4 \times 10^{21}$ cm^{-3} at the center of the ball, based on our ray-trace calculation assuming spherical symmetry on the ball [14]. Figure 2(b) shows a side-on x-ray pinhole image of self-emission at the shot of Fig. 2(a). The XRL-GIR system probed the plasma in the horizontal plane normal to the drilling beam, and the pinhole image was obtained from an angle of 45° in the vertical direction from the horizontal plane and 90° to the target normal. Two hot spots appeared in the x-ray image: one (hot spot *A*) is at 150 μm from the target surface and another (hot spot *B*) is on the target surface. The absolute position of hot spot *A* was determined by the x-ray cameras to be identical to that of the ball on the grid image in Fig. 2(a) and offset by 30 μm from the incident laser axis. The relation of both spots *A* and *B* could be seen slightly differently in Figs. 2(a) and 2(b) because of the difference in the observation angle of each diagnostics. Spot *A* has a 35 μm diameter (FWHM) with a spherical structure from the two x-ray pinhole camera images (front and side views), which is also consistent with the ball observed in Fig. 2(a). A part of the main beam may be stopped at near the critical density point, resulting in the density jump at the spot *A*. The density jump at near the critical density was reproducible at different focus positions of the main laser (e.g., 100 μm away from the target surface) [8]. More detail must be studied on the creation mechanism of this density jump in the future.

The second interesting distortions pointed out by *S* lines, which are key features in this paper, are seen as grid lines shifted away from the extrapolated lines of "*S*" arrows. The magnified image of the region around the main pulse interaction out of Fig. 2(a) is shown in Fig. 2(c). In order to clear the positions of the grid image elements, the grid image is shown with enhanced contrast. This type of grid shift is caused by the ridges of density humps such as plasma walls along the channel. Figure 3(a) shows the two dimensional density contour of the preplasma, while Fig. 3(b) shows the density contour plot of the plasma injected with the channeling beam corresponding to Fig. 2. The original center axis of the channeling laser beam is set at 0 μm in Fig. 3. The n_{cr} contour line in Fig. 3(a) has a smooth convex shape. The electron densities of the preplasma deduced from the XRL-GIR are extrapolated to be consistent with that from the UV interferometer [14]. The n_{cr} line in Fig. 3(b) is pulled inward by the injection of the channeling beam from the right hand side. The density well and the *S*-line density hump in the overcritical density regions were obtained only when large redshifts (>5 nm) were observed on the backscattered light spectra. The large redshifts were explained as a Doppler shift. The Doppler shift was caused when the channeling laser light was reflected from the vertex of the penetrating channel as described in Ref. [8]. The density humps along the *S* line should be created by the plasma evacuation radially from the channel due to the ponderomotive force. The evacuation results in a well and a cylindrical wall along the channel. The hot spot *B* in Fig. 2(b) was observed only when we observed the grid distortions (*S* lines) along the beam direction in Fig. 2(a) and large Doppler shifts on the backscattered spectra similar to the ones reported in Refs. [8] and [9]. The x rays from the hot spot *B* should be emitted when the channeling laser is terminated and

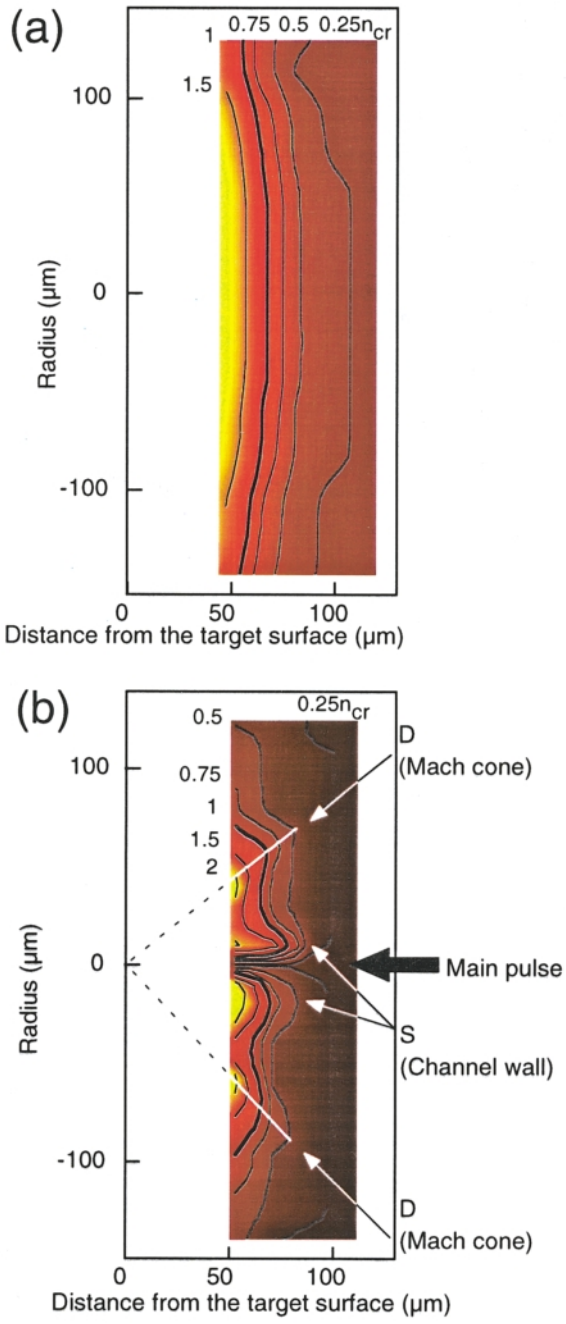

FIG. 3 (color). (a) Two dimensional image and contour of the preplasma obtained with the XRL-GIR system. The n_{cr} line has a smooth convex shape. (b) 2D image and contour of the plasma shown in Fig. 2(a). The graph was evaluated from the GIR picture in Fig. 2(a). The n_{cr} line is pulled inward by the channeling beam from the right.

absorbed in the overdense regions. A part of the channeling beam must push the critical density point with self-focusing into the overdense region.

Figure 4 shows the cross section of the electron density profile at a distance of 55 μm from the target surface in Fig. 3(b). The density well appears at a point close to the beam center and two kinds of density humps, shown by *S* and *D* arrows in Fig. 4, are seen on both sides of the density well. Any sudden change of the density gradient in the well made accurate density estimation difficult at the well bottom [16]. The width of the well is 30 ± 20 μm at 55 μm from the target surface. The electron density distribution in the well depends on the radial distribution of the laser ponderomotive force in the channel. A simple estimation is used based on an equilibrium condition between the thermal pressure $[k_B T_e (dn_e/dr)]$ and the ponderomotive force $(n_e f_p)$ [17]. Here T_e is the electron temperature, n_e is the electron density, r is the radial position, and f_p is the ponderomotive force. We assume the electron temperatures are between 1 and 10 keV and the laser energy losses in the channel are between 0% and 90%. Using both Gaussian and super-Gaussian (near rectangular) profiles as a radial intensity distribution of the laser light in the channel, the width of the laser intensity profile is calculated by $k_B T_e (dn_e/dr) = n_e f_p$ to be less than 30 μm in diameter (FWHM) for the Gaussian and 50 μm for the super-Gaussian. It is quite possible that this small diameter is maintained only by virtue of laser self-focusing. Thus we conclude that the figure captured a moment when the channeling laser beam self-focused into the preplasma well beyond the critical density.

Another density hump (*D* lines) appears at a greater radius from the channel walls shown by dotted lines in Fig. 3(b). The electron densities of the *D* line are 1.5–2 times higher than the background. The *D* lines merge at around the target surface where the hot spot *B* is observed. The divergence angles of the *D* lines are 45° relative to the beam axis. The channel front moves into the overdense region at a speed of 7×10^7 cm/s, which was estimated from Doppler shift of the backscattered light spectra [8]. Such a high speed of the channel front would generate a shock wave like a Mach cone. Assuming that the density hump is due to a Mach cone with an angle of 45° the plasma temperature is estimated to be about 3 keV corresponding to an ion sound speed of 5×10^7 cm/s [18]. Hydrodynamic simulation shows about a few keV at early time of the channel pulse that heats up the plasma without hole boring at an intensity of 10^{15} W/cm^2. Therefore, the *D*-line density hump could be due to a Mach cone created by the supersonic propagation of the channel front.

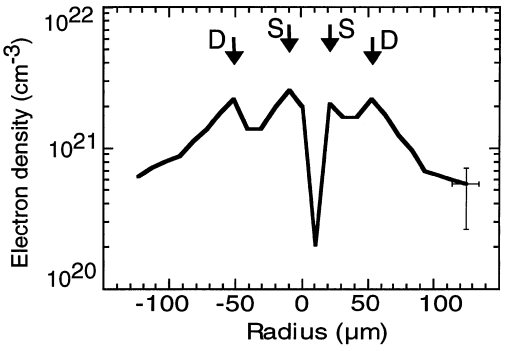

FIG. 4. Cross section of the density profile at 55 μm distance from the initial target surface in Fig. 3(b). The original center axis of the channeling beam is located at 0 μm on the horizontal axis.

We observed directly laser channeling into an overdense plasma using x-ray laser grid image refractometry (XRL-GIR) for the first time. The obtained picture and data reduction indicate laser beam self-focusing with a diameter of about 30 μm. We also observed the density perturbations exhibiting a 45° diverging angle which is consistent with a Mach cone created by the supersonic propagation of the channel front.

This work was performed with the technical support of Institute of Laser Engineering, Osaka University. We acknowledge the technical support on the target fabrication by Dr. M. Takagi and Ms. Y. Kimura. We acknowledge invaluable support by Dr. A. S. Wan at LLNL, Dr. H. Daido at ILE, Osaka University, and Dr. K. Murai at Osaka National Research Institute.

*Also at the Department of Electromagnetic Engineering, Osaka University, Yamada Oka 2-1, Suita, Osaka 565-0871, Japan.

[1] M. Tabak *et al.,* Phys. Plasmas **1**, 1626 (1994).
[2] A. Pukhov *et al.,* Phys. Rev. Lett. **79**, 2686 (1997).
[3] K. A. Tanaka *et al.,* Phys. Rev. E **60**, 3283 (1999).
[4] S. Wilks *et al.,* Phys. Rev. Lett. **73**, 2994 (1994).
[5] J. Fuchs *et al.,* Phys. Rev. Lett. **80**, 1658 (1998).
[6] P. E. Young, Phys. Plasmas **2**, 2815 (1995).
[7] R. Wagner *et al.,* Phys. Rev. Lett. **78**, 3125 (1997).
[8] R. Kodama *et al.,* Phys. Rev. Lett. **77**, 4906 (1996).
[9] K. Takahashi *et al.,* Opt. Commun. **135**, 45 (1997).
[10] D. Ress *et al.,* Science **265**, 514 (1994).
[11] L. B. Da Silva *et al.,* Phys. Rev. Lett. **74**, 3991 (1995).
[12] R. S. Craxton *et al.,* Phys. Fluids B **5**, 4419 (1993).
[13] T. Matsushita *et al.,* Institute of Laser Engineering Annual Report 1995, p. 183.
[14] R. Kodama *et al.,* Rev. Sci. Instrum. **70**, 543 (1999).
[15] R. Kodama *et al.,* Phys. Rev. Lett. **73**, 3215 (1994).
[16] The error bar in Fig. 4 shows the errors of absolute values of the electron densities. The profile error in Fig. 4 is much smaller than the absolute error value of the electron density. Therefore the density well and humps in Fig. 4 are obvious.
[17] F. F. Chen, *Introduction to Plasma Physics* (Plenum Press, New York and London, 1974).
[18] Mach cone angle θ is related to the Mach number M given by $\theta = \arcsin(1/M)$.